Mon. Not. R. Astron. Soc. **392,** 617–629 (2009) doi:10.1111/j.1365-2966.2008.14068.x

Evolution of the radio-loud galaxy population

E. Donoso,[1⋆] P. N. Best[2] and G. Kauffmann[1]

[1]*Max-Planck-Institut für Astrophysik, Karl-Schwarzschild-Str. 1, Postfach 1317, D-85741 Garching, Germany*
[2]*SUPA, Institute for Astronomy, Royal Observatory Edinburgh, Blackford Hill, Edinburgh EH9 3HJ*

Accepted 2008 October 8. Received 2008 October 8; in original form 2009 September 9

ABSTRACT

A catalogue of 14 453 radio-loud active galactic nuclei (AGN) with 1.4 GHz fluxes above 3.5 mJy in the redshift range $0.4 < z < 0.8$, has been constructed from the cross-correlation of the National Radio Astronomy Observatory Very Large Array Sky Survey (NVSS) and Faint Images of the Radio Sky at Twenty centimetres (FIRST) radio surveys with the MegaZ-luminous red galaxy (MegaZ-LRG) catalogue of LRGs derived from Sloan Digital Sky Survey imaging data. The NVSS provides accurate flux measurements for extended sources, while the angular resolution of FIRST allows the host galaxy to be identified accurately. New techniques were developed for extending the cross-correlation algorithm to FIRST detections that are below the nominal 1 mJy signal-to-noise ratio limit of the catalogued sources. The matching criteria were tested and refined using Monte Carlo simulations, leading to an estimated reliability of ∼98.3 per cent and completeness level (for LRGs) of about 95 per cent for our new catalogue.

We present a new determination of the luminosity function of radio AGN at $z \sim 0.55$ and compare this to the luminosity function of nearby ($z \sim 0.1$) radio sources from the Sloan Digital Sky Survey main survey. The comoving number density of radio AGN with luminosities less than 10^{25} W Hz^{-1} increases by a factor of ∼1.5 between $z = 0.1$ and 0.55. At higher luminosities, this factor increases sharply, reaching values of more than 10 at radio luminosities larger than 10^{26} W Hz^{-1}. We then study how the relation between radio AGN and their host galaxies evolves with redshift. Our main conclusion is that the fraction of radio-loud AGN increases towards higher redshift in all massive galaxies, but the evolution is particularly strong for the lower mass galaxies in our sample. These trends may be understood if there are two classes of radio galaxies (likely associated with the 'radio' and 'quasar mode' dichotomy) that have different fuelling/triggering mechanisms and hence evolve in different ways.

Key words: galaxies: active – galaxies: evolution – radio continuum: galaxies.

1 INTRODUCTION

Ever since the first studies of Longair (1966), it has been widely accepted that evolution is required to explain the radio source counts. Strong cosmological evolution of the high-luminosity radio source population has been established out to at least $z = 2$–3 (e.g. Dunlop & Peacock 1990), with the space densities of the most powerful radio sources increasing by a factor of $\sim 10^3$ relative to their densities at $z \sim 0$. However, the evolution of the low-luminosity radio galaxy population remained more uncertain. Clewley & Jarvis (2004) found that the low-luminosity population of radio sources with $L_{325\mathrm{MHz}} < 10^{25}$ W Hz^{-1}sr^{-1} exhibits no evolution out to $z \sim 0.8$. In contrast, Brown, Webster & Boyle (2001) found significant cosmic evolution out to $z \sim 0.55$, which they modelled using a pure luminosity evolution model as $P(z) = P(0)(1 + z)^{k_L}$, with $3 < k_L < 5$. More recently, similar results were obtained by Sadler et al. (2007), who analysed radio galaxies in the '2dF-SDSS Luminous Red Galaxy and Quasar' (2SLAQ) survey (Cannon et al. 2006). They found that the number density of radio sources below $P_{1.4\,\mathrm{GHz}} = 10^{26}$ W Hz^{-1} grows by a factor of ∼2 between $z = 0$ and 0.55. These results confirm that the cosmic evolution of low power radio sources is considerably weaker than that of their higher radio power counterparts. However, because of the relatively small sizes of samples, none of these studies was able to accurately constrain the luminosity dependence of the evolution.

Over the same period, our physical understanding of radio galaxies has developed steadily. Fanaroff & Riley (1974) showed that radio galaxies exhibit a dichotomy in radio morphology. Low radio luminosity sources are usually 'edge-darkened', with radio jets that quickly decelerate and flare as they advance through the interstellar medium (Fanaroff–Riley type I sources, or FR Is). In contrast, most

⋆E-mail: edonoso@mpa-garching.mpg.de

© 2008 The Authors. Journal compilation © 2008 RAS

higher luminosity sources have jets that remain relativistic over kpc and up to Mpc scales, ending in bright hotspots ('edge-brightened' sources, or FR IIs). The dividing line between FR Is and FR IIs occurs around a monochromatic power of $P_{1.4GHz} \sim 10^{25}$ W Hz^{-1}, although Ledlow & Owen (1996) showed that it occurs at higher radio luminosity in more optically luminous galaxies. This division is close to the break in the radio luminosity function, and has led to the hypothesis that these two populations of radio galaxies correspond to the different populations of cosmologically evolving sources, FR IIs being strongly evolving and FR Is much less so (e.g. Jackson & Wall 1999).

A more important division in the radio source population, however, appears to relate to the radiative properties of the active galactic nuclei (AGN). Powerful FR IIs and a small subset of the more powerful FR Is (e.g. see Heywood, Blundell & Rawlings 2007) show strong emission lines and either a visible or hidden quasar-like nucleus (Barthel 1989), indicative of radiatively efficient accretion. In contrast, most FR Is and a subpopulation of weak-emission-lined low-luminosity FR IIs show no evidence for a powerfully radiating nucleus (see Hardcastle, Evans & Croston 2007, and references therein) suggesting radiatively inefficient accretion. This implies that a fundamental difference exists between high and low power radio sources that is distinct from the radio morphological dichotomy. Instead, it is likely to be related to different origins or mechanisms of gas fuelling.

Understanding this low-luminosity radio source population, and its cosmic evolution, is not only important for understanding the physical origin of the radio activity, but also for understanding the galaxy evolution. There is growing evidence that low-luminosity radio-loud AGN play a critical role in regulating the masses and star formation rates of galaxies. Semi-analytic models of galaxy formation (e.g. see White & Frenk 1991 and Cole et al. 2000) successfully reproduce many of the observed properties of galaxies. However, these models overpredict the abundance of galaxies at the bright-end of the luminosity function. This problem arises because many massive galaxies are predicted to sit at the centre of hot hydrostatic haloes, in which cooling flows are expected to develop. If the gas cools and forms stars, central group and cluster galaxies are too massive by the present day and have much bluer colours than observed. Tabor & Binney (1993) first suggested that radio galaxies could, in principle, regulate these cooling flows, preventing significant accretion of gas and limiting the mass of galaxies. This concept of AGN feedback has now been successfully incorporated into the semi-analytic models of Bower et al. (2006) and Croton et al. (2006).

Observational support for a scenario in which radio AGN play an important role in regulating the growth of massive galaxies has slowly been accumulating. Both luminous FR IIs and low power FR Is can, in principle, inject a significant amount of energy into the surrounding gas, as their radio lobes expand and interact with the surrounding medium ($\sim 10^{42}$ erg^{-1} for the jets of a borderline FR I/FR II object, see Bicknell 1995). This has been directly observed in clusters of galaxies, where the expanding radio lobes create buoyant bubbles and drill cavities in the hot intracluster medium (Böhringer et al. 1993; McNamara et al. 2000; Fabian et al. 2003). In nearby systems, which can be studied in detail, the energy supplied by the radio source is well matched to that required to balance the cooling (e.g. Fabian et al. 2003).

With the availability of large redshifts surveys like the 2dF Galaxy Redshift Survey (2dFGRS, Colless et al. 2001) and the Sloan Digital Sky Survey (SDSS, York et al. 2000), it has become possible to obtain the sky and redshift coverage needed to define sufficiently large samples of nearby radio sources to study population statistics and global energetics. Best et al. (2005a) constructed a sample of 2215 radio-loud AGN brighter than 5 mJy with redshifts $0.03 < z < 0.3$ using the SDSS Data Release 2 (DR2) in combination with the National Radio Astronomy Observatory Very Large Array Sky Survey (NVSS, Condon et al. 1998) and the Faint Images of the Radio Sky at Twenty centimetres (FIRST, Becker, White & Helfand 1995). Best et al. (2005b) found that the fraction of radio-loud AGN, $f_{\rm RL}$, is a strong function of black hole and stellar mass, with dependencies $f_{\rm RL} \propto M_*^{2.5}$ and $f_{\rm RL} \propto M_{\rm BH}^{1.6}$. 25 per cent of the most massive galaxies (with $M_* \sim 10^{11.7}\,{\rm M}_\odot$) host radio sources more powerful than 10^{23} W Hz^{-1}. By combining these results with estimates of the energetic output of these sources, Best et al (2006) showed that the time-averaged mechanical energy output of radio sources in elliptical galaxies is comparable to the radiative cooling losses from the hot halo gas, for ellipticals of all masses. Radio sources can therefore provide sufficient energy to suppress cooling flows and regulate the growth of massive galaxies in the nearby Universe.

The role of powerful (radiatively efficient) FR II objects could not be addressed by Best et al. due to the scarcity of such systems in the low-redshift catalogue. Another open question is how the heating-cooling balance in massive galaxies evolves with redshift. In order to address these issues, we require a large radio galaxy sample at higher redshifts. In this paper, we extend the work of Best et al. by constructing a comparable catalogue of radio-loud AGN over the redshift range $0.4 < z < 0.8$. The catalogue contains a large number of luminous radio sources. By comparing with a sample of local radio sources selected from SDSS DR4, we aim to study not only the evolution of the radio galaxies, but also the evolution of the duty cycle of radio AGN activity in galaxies as a function of their stellar mass.

This paper is organized as follows. In Section 2, we will describe the surveys and samples used in this work, as well as the matching procedure. In Section 3, we will present results on the evolution of the radio luminosity function, radio-loud AGN fractions and the bivariate radio luminosity–stellar mass function, and the stellar mass and colour distributions of radio AGN host galaxies. Finally, we will summarize our results in Section 4 and discuss the implications of our work. In this paper, the adopted values for the cosmological parameters are $\Omega_{\rm m} = 0.3$, $\Omega_\Lambda = 0.7$ and $\rm H_0 = 70\,km\,s^{-1}\,Mpc^{-1}$.

2 THE RADIO-OPTICAL GALAXY SAMPLES

2.1 The MegaZ-LRG Galaxy catalogue

The SDSS (York et al. 2000; Stoughton et al. 2002) is a five-band photometric and spectroscopic survey that has mapped almost a quarter of the whole sky, providing precise photometry for more than 200 million objects and accurate redshifts for about a million galaxies and quasars. Imaging data in the *ugriz* bands (Fukugita et al. 1996) has been obtained with a large format CCD camera (Gunn et al. 1998) mounted on a dedicated telescope located at Apache Point Observatory in New Mexico. Astrometric coordinates are accurate to ~0.1 arcsec per coordinate. Throughout this work, unless otherwise stated, all magnitudes are model magnitudes, derived from the best-fitting de Vaucouleurs or exponential profile in the *r* band. The amplitude is then scaled to fit measurements in other filters. This provides the best estimate of galaxy colours since the same aperture is used in all passbands. A correction for foreground Galactic extinction is applied to all the magnitudes following Schlegel, Finkbeiner & Davis (1998).

The MegaZ-LRG (Collister et al. 2007) is a photometric redshift catalogue based on imaging data from the fourth Data Release (DR4) of the SDSS. It consists of ∼1.2 million luminous red galaxies (LRGs) with limiting magnitude $i < 20$ over the redshift range $0.4 < z < 0.8$. MegaZ adopts various colour and magnitude cuts to isolate red galaxies at $0.4 < z < 0.8$. The cuts are very similar to those adopted by the '2SLAQ' project (Cannon et al. 2006). The specific colour cuts are

$$0.5 < g - r < 3, \quad (1)$$

$$r - i < 2, \quad (2)$$

$$c_{\rm par} \equiv 0.7(g - r) + 1.2(r - i - 0.18) > 1.6, \quad (3)$$

$$d_{\rm perp} \equiv (r - i) - (g - r)/8 > 0.5. \quad (4)$$

Essentially, $c_{\rm par}$ isolates early-type galaxies (LRGs), while $d_{\rm perp}$ selects galaxies with redshifts $z > 0.4$. Accurate photometric redshifts are available for the entire LRG sample. These are derived using a neural network photometric redshift estimator (ANNZ, Collister & Lahav 2004). The neural net was trained using a sample of ∼13 000 LRGs with spectroscopic redshifts from 2SLAQ. The rms average photometric redshift error for all the galaxies in the sample is $\sigma_{\rm rms} = 0.049$.

2.2 The NVSS and FIRST radio catalogues

The NVSS (Condon et al. 1998) is a radio continuum survey at 1.4 GHz, covering the whole sky at declinations $\delta_{\rm J2000} > -40^\circ$. The survey provides total intensity and polarization measurements down to a limiting point source flux density of ∼2.5 mJy. The rms noise and confusion limit in the total intensity maps is $\sigma_{\rm rms} \approx 0.45$ mJy beam^{-1}, except near very strong sources. The survey was carried out using the Very Large Array (VLA) in compact D and DnC configurations, which provides an angular resolution of around 45 arcsec. A catalogue of ∼1.8 million point sources was derived by fitting elliptical Gaussians to the discrete peaks in the images. The catalogue lists peak flux densities and best-fitting sizes for all sources with fluxes $S_{\rm peak} \geq 2$ mJy beam^{-1}. The completeness of the NVSS is around 50 per cent at ∼2.5 mJy, but rises sharply to more than 99 per cent at 3.5 mJy.

The VLA FIRST (Becker et al. 1995) is a survey that covers 10 000 deg^2 of the North Galactic Cap, using the VLA in its B configuration at 1.4 GHz. This delivers a resolution of ∼5 arcsec and a typical noise of $\sigma_{\rm rms} \approx 0.13$ mJy, except in the vicinity of bright sources (>100 mJy), where sidelobes can lead to an increased noise level. The sky coverage overlaps most of the SDSS in the Northern Galactic Cap. As with the NVSS, a source catalogue including peak and integrated flux densities and sizes was derived from fitting a two-dimensional Gaussian to each source generated from the co-added images. Astrometric accuracy in this source catalogue is better than 1 arcsec for the faintest sources detected at the nominal threshold of 1 mJy.

2.3 Identification of radio-loud AGN

The NVSS and FIRST surveys are highly complementary in many respects. NVSS has sufficient surface brightness sensitivity to provide accurate flux measurements of extended radio sources with lobes and jets. On the other hand, the superior angular resolution of FIRST is necessary to identify the central core component of the radio sources and associate it with the host galaxy detected in optical surveys.

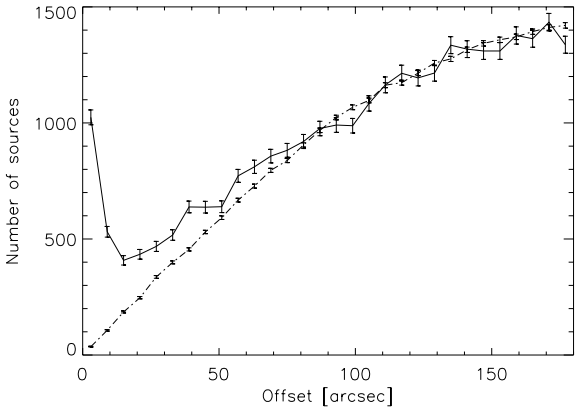

Figure 1. Distribution of offsets between the MegaZ-LRG galaxies and the closest NVSS source (solid line) and the corresponding offset distribution derived from the random samples (dot–dashed line). Most true matches clearly stand out at offsets less than 15 arcsec, but the excess remains significant out to separations of ∼70 arcsec.

Best et al. (2005a) developed an automated hybrid cross-matching method to identify radio galaxies in the SDSS DR2. The method made use of both NVSS and FIRST, thereby exploiting the advantages of each survey and avoiding the errors that arise by using them separately. A collapsing algorithm was used to identify multiple-component FIRST and NVSS sources. The final catalogue consisted of 2712 radio galaxies brighter than 5 mJy (2215 radio-loud AGN and 447 star-forming galaxies). The reliability and completeness of the catalogue was estimated to be 98.9 and 95 per cent, respectively.

This paper presents an extension of the Best et al. (2005a) method by combining NVSS and FIRST with the high-redshift MegaZ-LRG catalogue. We largely follow the procedure described in Best et al. (2005a), but a few small modifications were implemented in order to accommodate the characteristics of the new sample. The changes were tested and progressively refined using a set of 10 Monte Carlo simulations of a 720 deg^2 patch of the survey area. The numbers quoted in the description below pertain to this small test area.

(i) Best et al. (2005a) considered radio sources above a limit of 5 mJy. The major reason for this choice was to reduce any loss of sensitivity to multicomponent NVSS sources. The MegaZ radio sources are more distant and their angular sizes are thus smaller, so there are fewer multicomponent sources (see Section 2.5). In order to probe fainter radio galaxies out to higher redshifts, we adopted a flux limit of 3.5 mJy. This limit corresponds to approximately seven times the noise level in the NVSS maps.

(ii) Fig. 1 shows the distribution of positional offsets between the SDSS LRG and the nearest NVSS match, for galaxies not classified as multicomponent NVSS sources. There is a clear excess of galaxies compared to random matches for separations less ∼10–15 arcsec. The excess remains significant out to ∼70 arcsec. A significant part of the effect at larger angular separations is because galaxies are intrinsically clustered (see discussion in Best et al. (2005a) and also Section 2.5). However, some part may consist of true associations between LRGs and extended NVSS sources. The subsequent FIRST cross-matching helps us pinpoint such cases. Best et al. (2005a) carried out this cross-matching for all SDSS galaxies with a single-component NVSS match within 30 arcsec.

© 2008 The Authors. Journal compilation © 2008 RAS, MNRAS **392,** 617–629

In this work, this limit is increased to 60 arcsec. This identifies an extra 37 (2.8 per cent) genuine radio galaxies at a cost of 0.8 false matches, i.e. a decrease in reliability of only ∼0.01 per cent.

(iii) Because the NVSS radio sources reach a fainter limit than those studied by Best et al. (2005a), we find more objects (∼8 per cent) with no FIRST match. These are likely to be extended sources missed by the low surface brightness sensitivity of FIRST, but a small fraction may be the variable radio sources whose flux density has changed between observations. A careful inspection of FIRST images (along with NVSS and SDSS cutouts) around the positions of these objects revealed that in many cases there were bright spots near or slightly below the survey flux limit, which were clearly associated with a MegaZ optical galaxy. A method to use this information to increase the number of matches was developed and tested. The details are explained in the following section.

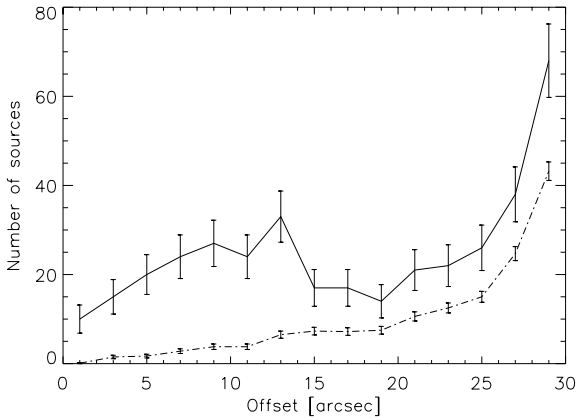

Figure 2. Distribution of offsets between MegaZ-LRG galaxies and NVSS candidates for sources that have no match in the FIRST catalogue. Results are shown for real (solid line) and random (dot–dashed line) samples. Matches with separations larger than ∼15 arcsec are mostly the result of galaxy clustering.

2.4 Improved matching of sources without FIRST counterparts

The high resolution of the FIRST survey is essential to allow reliable cross-matching with dense optical samples. The NVSS sources without FIRST counterparts are the largest source of incompleteness in the final sample (see Best et al. 2005a). However, blindly accepting all LRG candidates out to a separation of 20 arcsec from the NVSS source introduces an average of 42.2 false detections in our random samples, reducing the reliability of the catalogue to 79 per cent within our test area (see Fig. 2, where the distribution of NVSS-MegaZ offsets is plotted for real and random data).

We turned to the analysis of the FIRST radio maps around the candidate positions, in order to retain as many of these sources as possible without introducing significant contamination. Fig. 3 shows FIRST cutouts of typical objects with no catalogued FIRST source, but with a nearby NVSS-MegaZ association. In many cases, one or more bright 'spots' matching the NVSS source and MegaZ galaxy can be seen, while in some cases two well-defined symmetric radio lobes centred around the optical galaxy are evident.

We took advantage of this additional information in deciding whether candidates should be accepted as true FIRST matches. For galaxies within 10 arcsec of the NVSS source we accepted all matches, following Best et al. (2005a). In the test area, this provided 96 associations of which 9.9 are expected to be false (i.e. 10.3 per cent contamination). For galaxies with offsets between 10 and 15 arcsec, we accepted matches according to the following procedure.

(i) The FIRST image was segmented using an initial threshold of $3\sigma_{\rm rms}(\alpha, \delta)$, where $\sigma_{\rm rms}(\alpha, \delta)$ is the *local* rms noise in the map.

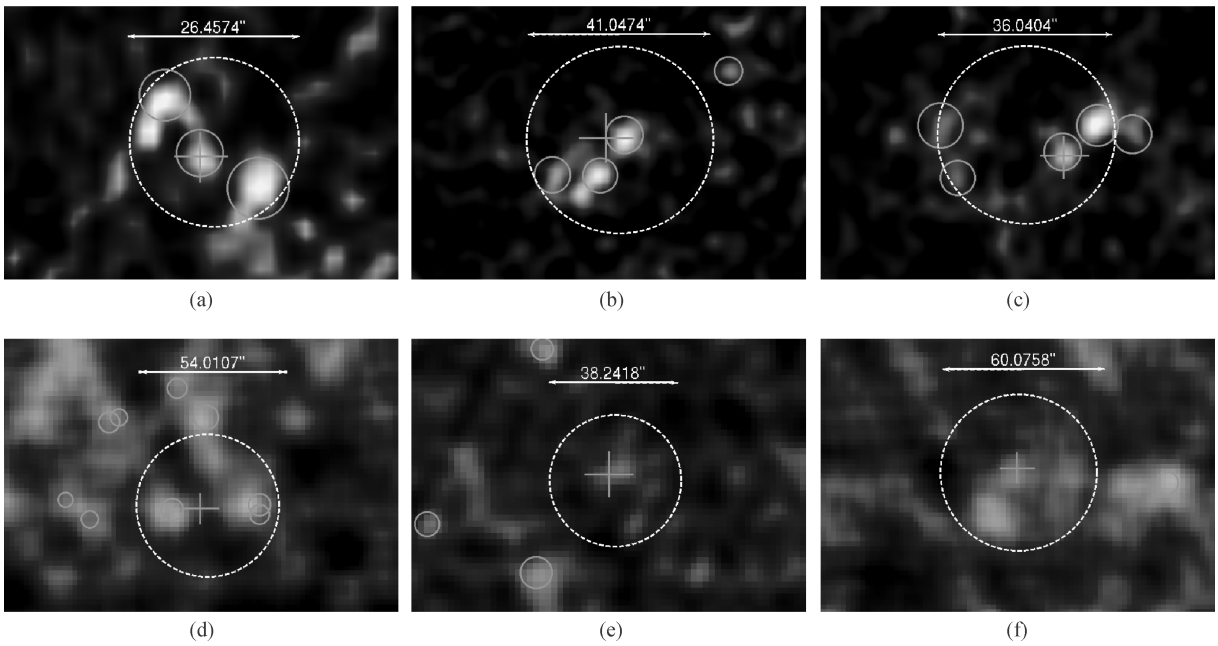

Figure 3. FIRST cutouts around sources without FIRST counterparts. The dashed circle marks the NVSS source position and size, while the plus sign indicates the MegaZ optical galaxy location. The small circles mark the detected spots. Cases (a), (b) and (c) are examples of accepted matches and cases (d), (e) and (f) are examples of rejected ones. A boxcar sliding average filter has been applied to enhance the visibility.

Table 1. Numbers of different classes of accepted MegaZ-LRG radio galaxies, as well as the corresponding numbers found in the random samples. The numbers are for a 720 deg^2 patch of the total survey area. Values in parentheses indicate the number of sources accepted using the spot-matching technique (see the text).

NVSS type	FIRST type	MegaZ	Random	Reliability (per cent)
NVSS single	0 component	109 (13)	12.3 (2.4)	88.7
NVSS single	1 component	1068	7.8	99.3
NVSS single	2 components	88	1.2	98.7
NVSS single	3 components	38	0.3	99.2
NVSS single	4+ components	6	0.1	98.3
NVSS multiple		24	0.8	96.7
Total		1333	22.5	98.3

This provided a number of seed spots whose centroids were refined using the intensity-weighted moments in both the directions.

(ii) A brightness profile was derived for each spot and both the half light radius and the flux inside this radius were determined.

(iii) Any bright spot with a mean flux density greater than 0.4 mJy and within 5 arcsec of the optical counterpart was considered to be a valid match. These sources were accepted unless there were more than four bright spots inside a circle of 30 arcsec, in which case the match was rejected because it is then impossible to associate the source with a single MegaZ galaxy. Visual inspection of SDSS images confirmed this.

To test this 'spot matching' technique, we repeated the same procedure for matches without FIRST components in the random samples. This constitutes a robust check, since we are in effect looking at random locations in the sky, so we can assess how probable it is to find a spot pattern by chance. In the sky test area, our procedure identified 13 additional FIRST for sources with NVSS-MegaZ offsets between 10 and 15 arcsec, at the cost of introducing only 2.4 false detections. This increases the overall completeness of the sample, for little cost in reliability. Our tests indicate that it is not possible to extract more matches beyond a ∼15 arcsec offset with reasonable confidence.

2.5 Reliability, completeness and final catalogue

Table 1 lists the number of accepted radio matches for different classes of radio sources found in the sky test area. We provide results for both the real and random samples, as well as reliability estimates. Note that even though our sample is much deeper and more than five times larger than the one of Best et al. (2005a), we have been able to compile a catalogue with comparable reliability (∼98.3 per cent).

Because the true number of radio sources is unknown, the completeness is more difficult to estimate than reliability. Nevertheless, a reasonable estimate of the completeness can be obtained by considering the MegaZ-LRGs that have a NVSS source within a distance of 15 arcsec. These can be assumed to be a mixture of true matches, random alignments from sources at different redshifts and a contribution from sources that are associated with other galaxies which just happen, through clustering, to be close to the target galaxy. By using the Monte Carlo simulations in the sky test area to estimate the latter two contributions, we can estimate the number of true matches and hence the completeness.

In the sky test area, there are 1765 MegaZ-LRGs with a NVSS source within a distance of 15 arcsec. In comparison, there are an average of 225 sources within the same distance to the galaxies in the random catalogues. Determining the contribution from clustered galaxies is more complicated. We attempted this in two ways.

First, we selected all NVSS–SDDS candidates with a single FIRST component within 15 arcsec, but which were rejected by the matching algorithm. We then searched for other optical MegaZ galaxies in a 3 arcsec region around these FIRST radio positions (a standard search radius for FIRST matching, e.g. Obric et al. 2006). From a total of 359 LRGs, 40 (11.1 per cent) had a nearby LRG with an associated FIRST source. The corresponding fraction in the random sample was 0 per cent. This means 11.1 per cent of the 1765 sources (∼200) within 15 arcsec are due to clustering.

To check this result, we estimated the excess number of LRG–LRG pairs over random by integrating the angular correlation function $w(\theta)$ given by Ross et al. (2007) for the 2SLAQ catalogue out to 15 arcsec. This yielded value of 1.66, i.e. ∼150 extra sources due to clustering. These two values are in rough agreement; the fact that the first method gives a slightly larger number could be explained by the fact that radio galaxies are more massive than the underlying LRG population, so we would expect them to be more strongly clustered. For our final completeness estimate, we will assume that 180 sources are due to clustering.

The expected number of true matches is then estimated as $1765 - 225 - 180 = 1360$. Our matching procedure detects 1309 objects, of which 21.7 are predicted to be false detections. The completeness can therefore be estimated as 100(detected − false)/expected or $100(1309 - 21.7)/1360 \approx 95$ per cent. This value is comparable to that obtained by Best et al. (2005a), for a much lower redshift sample. We note that this completeness estimate applies only to the MegaZ-LRG sample and does not take into account missing radio-loud quasi-stellar objects or radio galaxies that do not meet the MegaZ-LRG colour cuts. [1]

Table 2 lists the final number of radio galaxies found in the MegaZ-LRG sample and included in the catalogue. Our catalogue is by far the largest sample of radio galaxies of its kind. Out of a total of 14 553 sources, the majority (78.6 per cent) have single counterparts in both FIRST and NVSS. A significant fraction (11.5 per cent) is resolved by FIRST into multiple components. Only 253 (1.7 per cent) sources have multiple NVSS counterparts, to be compared with the 6.2 per cent found by Best et al. (2005a). This is again expected, because the radio galaxies lie at larger distances.

[1] A preliminary comparison with a complete spectroscopic catalogue at similar redshifts indicates that ∼20 per cent of all galaxies with $M_* > 10^{11}$ M$_\odot$ are too blue to fall within the MegaZ-LRG colour boundaries. Since radio AGN are biased towards the higher mass galaxies, the corresponding percentage should be smaller for this population.

© 2008 The Authors. Journal compilation © 2008 RAS, MNRAS **392,** 617–629

Table 2. Total number of MegaZ-LRG radio galaxies with 1.4 GHz flux above 3.5 mJy in the different classes.

NVSS type	FIRST type	MegaZ
NVSS single	0 component	1176
NVSS single	1 component	11 445
NVSS single	>1 components	1679
NVSS multiple		253
Total		14 453

We note that as for Best et al. (2005a), a fraction of the candidate sources (1093 objects, or 7.5 per cent of the sample) with multiple NVSS or FIRST components were flagged as being too unreliable to classify by automated means. These were classified visually by simultaneous examination of SDSS, NVSS and FIRST images. Of these, 221 were accepted as genuine sources. Finally, to ensure that the same NVSS source was not associated with two different MegaZ-LRG galaxies, the complete catalogue was checked. Such duplications arose for 560 candidates and all cases were visually examined. Altogether, 564 positive matches (3.9 per cent) result from the visual classification process.

Finally, we note that it is important to distinguish between stars and galaxies when compiling the radio galaxy catalogue, because late M-type stars have colours that are very similar to those of faint LRGs. Collister et al. (2007) used the same neural network technique used to derive photometric redshifts, to perform star/galaxy separation. The neural net was given 15 different photometric parameters and trained using the 2SLAQ spectroscopic sample. The MegaZ catalogue provides a parameter, $\delta_{\rm sg}$, which is the probability that a particular object is a galaxy rather than a star. In the subsequent analysis, we only consider objects with $\delta_{\rm sg} > 0.7$ (99.93 per cent of all the matched radio galaxies, 96.78 per cent of all optical galaxies).

2.6 Comparison sample

In the following sections, we will compare the results obtained for the MegaZ-LRG catalogue of radio AGN to those obtained for galaxies selected from the main spectroscopic galaxy sample, which have redshifts in the range $0.01 < z < 0.30$, with a mean redshift of $\langle z \rangle \sim 0.14$. This is an extension to the fourth data release of the original DR2 radio-matched catalogue of Best et al. (2005a).

3 RADIO-LOUD AGN EVOLUTION

3.1 Masses and $(K + e)$-corrections

To derive stellar masses for each galaxy, we used the KCORRECT algorithm (Blanton & Roweis 2007), which finds the non-negative linear combination of spectral templates that best match the flux measurements of each galaxy in a χ^2 sense. These templates are based on a set of Bruzual & Charlot (2003) models and span a wide range of star formation histories, metallicities and dust extinction, so they can be used to estimate the mass-to-light ratio of a galaxy. This method yields stellar masses that differ by less than 0.1 dex on average from estimates using other techniques, for example using the 4000 Å break strength and $H\delta$ absorption index to estimate M/L as proposed by Kauffmann et al. 2003.

In order to compare radio galaxies at different redshifts in a fair way, we need to compute the volume over which the MegaZ sources

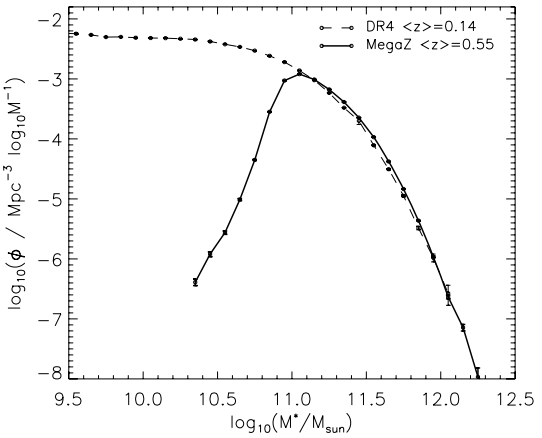

Figure 4. Mass function for galaxies in the MegaZ-LRG (solid thick line) and the DR4 sample (dashed thin line).

are visible, given the magnitude and colour cuts of the surveys as well as the 3.5 mJy radio flux limit. In this work, we generated $(K + e)$-corrections using a library of Bruzual & Charlot (2003) evolutionary stellar population synthesis models. LRGs constitute a nearly homogeneous population of old, red, early-type galaxies with spectral energy distributions that are reasonably well described by a single stellar population (SSP) model that forms all its stars in an instantaneous burst at high redshifts (we choose $z = 9.84$) and then passively evolves (Wake et al. 2006). We use these models to compute K-corrections, which account for the redshifting of the spectra through the different rest-frame bandpasses, and e-corrections, which account for the intrinsic evolution in the spectral energy distribution of galaxies because stars are younger at higher redshifts. With these corrections in hand, we are able to predict the u, g, r, i, z magnitudes as well as the radio luminosities of each MegaZ-LRG as function of redshift, which then allows us to determine the precise minimum ($z_{\rm min}$) and maximum ($z_{\rm max}$) redshift that a particular object enters and then leaves the radio-optical sample. The weight for each galaxy is then $1/V_{\rm max}$, where $V_{\rm max}$ is the integral of the comoving volume between $z_{\rm min}$ and $z_{\rm max}$.

As a check, we have computed the stellar mass function of the LRGs in the MegaZ catalogue and we compare our results with stellar mass function of low-redshift massive galaxies drawn from DR4. This is shown in Fig. 4. The MegaZ-LRG sample probes the high-mass end of the stellar mass function, spanning a range in stellar mass from 10^{11} to $10^{12.1}$ $\rm M_{\odot}$. Over this range in mass, there is essentially no evolution in the stellar mass function out to $z \sim 0.55$. This is in accord with recent results presented by Brown et al. (2007) and Cool et al. (2008), who show that the upper end of the stellar mass function has apparently changed very little out to a redshift of $z \sim 0.9$.

3.2 Radio luminosity function

A standard technique for quantifying the rate of evolution of a population of galaxies is to compare the radio luminosity function of these objects at two different epochs. In this section, we will determine the evolution of the radio-loud AGN population by comparing the luminosity function of MegaZ-LRG radio galaxies with that derived from the SDSS DR4 sample.

These functions were calculated for radio sources above a 1.4 GHz flux density limit of 3.5 mJy using the standard $1/V_{\rm max}$ formalism (Schmidt 1968). We estimate $V_{\rm max}$ for each galaxy as

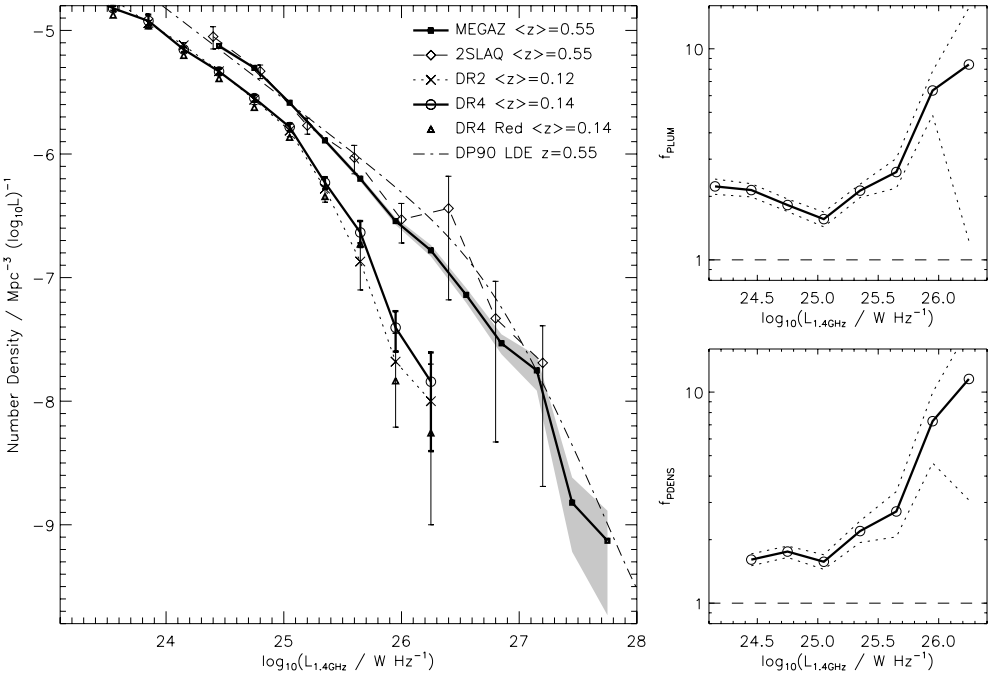

Figure 5. The radio luminosity function at 1.4 GHz derived for MegaZ-LRG and DR4 samples (thick line with square and circle symbols, respectively). An additional DR4 RLF restricted only to red-sequence galaxies (triangles) is also plotted. Likewise shown are the calculations by Sadler et al. (2007) for 2SLAQ (thin line and diamond symbols), and by Best et al. (2005a) for SDSS DR2 (dashed line and crosses). Results are in good agreement at both redshift intervals. The luminosity function based on the luminosity/density evolution model of Dunlop & Peacock (1990) is also overplotted (dash–dotted line). The right-hand panels show the factors by which luminosity and density should increase in order to match the DR4 curve at $\langle z \rangle \sim 0.14$ with the MegaZ-LRG curve at $\langle z \rangle \sim 0.55$. No evolution scenarios are indicated by the horizontal dashed lines. Error bars are poissonian, except for the right-hand upper panel where they are calculated via statistical bootstrapping of each sample.

the maximum comoving volume within which it would be visible given the radio flux and optical magnitude limits and the colour cuts used to define the MegaZ-LRG sample (see Section 2.1). We have included both *K*-corrections and *e*-volutionary corrections in this computation. These corrections were described in the previous section. Radio luminosities are calculated using the formula

$$\log_{10}[\mathrm{P}_{1.4\,\mathrm{GHz}}] = \log_{10}[4\pi \mathrm{D}_{\mathrm{L}}^2(\mathrm{z})\mathrm{S}_{1.4\,\mathrm{GHz}}(1+\mathrm{z})^{\alpha-1}], \quad (5)$$

where $\mathrm{D_L}$ is the luminosity distance in the adopted cosmology, $\mathrm{S}_{1.4\,\mathrm{GHz}}$ is the measured radio flux, $(1 + \mathrm{z})^{\alpha-1}$ is the standard *k*-correction used in radio astronomy and α is the radio spectral index ($S_\nu \propto \nu^{-\alpha}$) for which we adopted a value of 0.7, as is usually assumed for radio galaxies (Condon, Cotton & Broderick 2002).

The normalization of the luminosity function requires knowledge of the precise intersection area of all three surveys: NVSS, FIRST and the SDSS DR4 photometric sample. We used the footprint services of the Virtual Observatory[2] (Budavári et al. 2006) to derive a total area of 6164.6 deg^2. A further 8.3 deg^2 was subtracted to avoid noisy regions around bright NVSS sources, resulting in an effective area of 6156.3 deg^2. In the MegaZ sample, the maximum variation of the mean redshift as we go from our second luminosity bin to the highest luminosity one, is ∼0.025. If we include the first bin, this difference increases to a value ∼0.08. We nevertheless decide to keep the lowest luminosity bin to avoid introducing further luminosity cuts.

In Fig. 5, we plot the radio luminosity function measured for the MegaZ-LRG catalogue and the results are also tabulated in Table 3.

[2] http://www.voservices.net/footprint

Table 3. The MegaZ-LRG luminosity function for radio-loud AGN at 1.4 GHz.

$\log_{10}(\mathrm{P}_{1.4\,\mathrm{GHz}})$ (W Hz^{-1})	$\log_{10}(\rho)$ (Mpc^{-3} (log$_{10}$ L)$^{-1}$)	N
24.45	$-5.13^{+0.02}_{-0.02}$	2218
24.75	$-5.30^{+0.01}_{-0.01}$	5438
25.05	$-5.59^{+0.01}_{-0.01}$	3506
25.35	$-5.89^{+0.02}_{-0.02}$	1742
25.65	$-6.20^{+0.02}_{-0.02}$	840
25.95	$-6.54^{+0.03}_{-0.03}$	365
26.25	$-6.78^{+0.04}_{-0.05}$	185
26.55	$-7.14^{+0.06}_{-0.06}$	87
26.85	$-7.53^{+0.07}_{-0.09}$	41
27.15	$-7.75^{+0.12}_{-0.16}$	18
27.45	$-8.82^{+0.20}_{-0.40}$	3
27.75	$-9.13^{+0.24}_{-0.60}$	1

For comparison, we reproduce the luminosity function calculated by Sadler et al. (2007) for the 2SLAQ LRG sample. There is very good agreement, but our new determination has considerably smaller error bars, because our sample is very much larger. This is especially important for determining the number density of radio sources with radio powers greater than $\mathrm{P}_{1.4\,\mathrm{GHz}} = 10^{26}$ W Hz^{-1}. Also plotted in the figure are two determinations of the radio luminosity function from SDSS DR4: the first without colour restrictions, and the second restricted to red galaxies as defined by a luminosity-dependent $g - r$

colour cut found by fitting bi-Gaussian functions to the distribution of $g - r$. The details of the method are explained by Li et al. (2006). For reference purposes, we also show the radio luminosity function (RLF) obtained by Best et al. (2005a) for the DR2 sample.

The evolution of the luminosity function of a population of objects is often characterized in terms of simplified density or luminosity evolution models. In a pure density evolution model, the underlying luminosity distribution of the radio sources remains fixed, but the number density of the sources increases at higher redshifts. This might be the case if a larger fraction of galaxies harbour radio jets at higher redshifts, but the intrinsic properties of the jets do not evolve with time. In a pure luminosity evolution model, there is a fixed population of radio AGN with luminosities that dim as the radio sources age.

In the two right-hand panels of Fig. 5, we plot the ratios $f_{\rm PDENS}$ and $f_{\rm PLUM}$ as a function of radio luminosity. $f_{\rm PDENS}$ is the ratio of the comoving number densities of radio sources in the MegaZ and DR4 catalogues at fixed radio luminosity, while $f_{\rm PLUM}$ is the factor by which the low-redshift number densities should grow in order to match the values found at higher redshift. If either model is a correct description of the data, one should find constant f values as a function of radio luminosity. We find that neither model is a good description of the data. Both plots show a sharp increase near $\rm P_{1.4\,GHz} \sim 10^{25}$ W Hz^{-1}.

In Fig. 5, we also plot the radio luminosity function for steep-spectrum sources at $z = 0.55$ predicted by the luminosity/density evolution model of Dunlop & Peacock (1990). This model is based on high-frequency data, and has been shown to provide an accurate description of the radio source counts and redshift distributions. At the redshifts corresponding to our MegaZ-LRG sample, the models were only strongly constrained above 10^{26} W Hz^{-1} due to the high flux limits of their radio samples, and were then extrapolated to the lower radio powers. We note that Dunlop & Peacock (1990) provide a range of different parametrizations in their paper, but all give very similar results at moderate redshifts. As can be seen, our data match the Dunlop & Peacock (1990) model reasonably well. In particular, the extrapolation to lower radio power appears to provide a reasonable fit to our data, but our estimate appears to be 0.2–0.3 dex lower than that of Dunlop & Peacock (1990) over the luminosity range from 10^{25} to $10^{26.5}$ W Hz^{-1}.

It is important to note that if radio galaxies fall outside the MegaZ-LRG colour selection criteria, they will be missed in our radio luminosity function determination. Such an effect is visible for our low-redshift luminosity function at radio powers above 10^{26} W Hz^{-1}; the luminosity function of bright sources in the red galaxy population is 0.1–0.2 dex lower than for the DR4 sample as a whole. Neither the DR4 sample nor the MegaZ-LRG sample includes radio-loud quasars, which would likely increase the amplitude of the radio luminosity functions by $\sim$0.1 dex above a radio luminosity of 10^{25} W Hz^{-1}. Nevertheless, it is clear from our comparisons that a large fraction (i.e. >50 per cent) of all radio galaxies at $z = 0.55$ do reside in the LRG population. In the rest of the paper, we will be comparing radio AGN *fractions* at low and high redshifts, and we will show that such fractional estimates are much less sensitive to any incompleteness in our sample.

3.3 Fraction of radio-loud AGN

We are now in a position to investigate the relation between radio-loud AGN and their host galaxies. Over the redshift range covered by the MegaZ-LRG sample ($0.4 < z < 0.8$), radio sources have 1.4 GHz powers well above 10^{24} W Hz^{-1} (the faintest radio galaxies in our sample are $\sim 10^{24.4}$ W Hz^{-1}). It is well known that radio emission above this luminosity is rarely associated with star formation, but rather an AGN (Sadler et al. 2002; Best et al. 2005a). In addition, LRGs are photometrically defined so that the majority of star-forming galaxies are excluded, so we can safely assume that our sample is dominated by an AGN population. Fig. 6 shows the fraction of MegaZ-LRGs with radio luminosities above different thresholds, as a function of their stellar mass. The fraction of LRGs with radio AGN more luminous than $10^{24.4}$ W Hz^{-1} rises from $\sim$0.04 per cent, for galaxies with stellar masses around $10^{10.8}\ M_{\odot}$, to $\sim$25 per cent, for the most massive LRGs with $M_* \sim 10^{12.2}\ M_{\odot}$. Results for radio power cuts of 10^{25} W Hz^{-1}, $10^{25.5}$ W Hz^{-1} and 10^{26} W Hz^{-1} are also included in the plot and a similar mass dependence is found. The dotted lines connecting light symbols on the plot show the corresponding dependence of the radio-loud fraction on stellar mass for the low-redshift SDSS DR4 sample. We find that there is an increase in higher redshifts in the fraction of radio-loud AGN hosted by galaxies of all stellar masses. The increase is larger at higher radio luminosities and for galaxies with lower stellar masses. This is shown in more detail in the bottom three panels of Fig. 6, where we plot the relative ratio δf between the high- and low-redshift data [$\delta f = (f_{\rm MegaZ} - f_{\rm DR4})/f_{\rm DR4}$] as a function of mass and for our three radio luminosity thresholds.

Once again it is important to recall that the DR4 sample includes all galaxies regardless of colour, whereas the MegaZ sample is restricted to red galaxies. Best et al. (2005b) showed that the probability for a galaxy to host a radio-loud AGN was not influenced by its stellar population. In the top right-hand panel of Fig. 6, we compare the radio-loud AGN fraction versus mass relation for the full DR4 sample to the results obtained if the sample is restricted to galaxies with $g - r$ colours greater than 0.8. As can be seen, the results are almost identical. The effect of the colour cut is much smaller than the evolutionary trends we find between the low redshift and MegaZ-LRG sample.

To check whether the increase in the fraction of radio-loud AGN with mass is not simply the result of the fact that more massive galaxies harbour more massive black holes and hence produce more radio emission, we have also calculated the fraction of radio-loud AGN that are above a given limit in radio luminosity per unit stellar mass. For our sample, this is equivalent to choosing only those sources that produce radio emission above a fixed fraction of the Eddington limit. For reasonable values of the chosen limit (e.g. $L/M^* > 10^{13.3}$ W Hz^{-1} M$^{-1}{}_{\odot}$), the strong mass dependences persist, although the slope of the relation is somewhat shallower.

It is also important to check if the small percentage of galaxies that might be misclassified due to random superposition ($\sim$1.7 per cent, see Section 2.5) could affect these results. As $\sim$1.2 per cent of objects in MegaZ are radio loud, only 0.02 per cent of galaxies might be false matches. For the most massive systems, such contribution to the radio-loud fraction is negligible. For low-mass galaxies around $10^{10.9}\,\rm M_{\odot}$, only $\sim$0.1 per cent are radio loud, so that the error due to false detections is at most 20 per cent, a value that is well below the observed change factors of 2–5 in evolution.

3.4 Other systematic effects

Photometric redshift codes have improved vastly over the years and the resulting redshift estimates are useful for a broad range of studies. Even though the neural network photometric redshift estimator used in the MegaZ catalogue has been through fully calibrated using spectroscopic redshifts, it is important to test the sensitivity of our

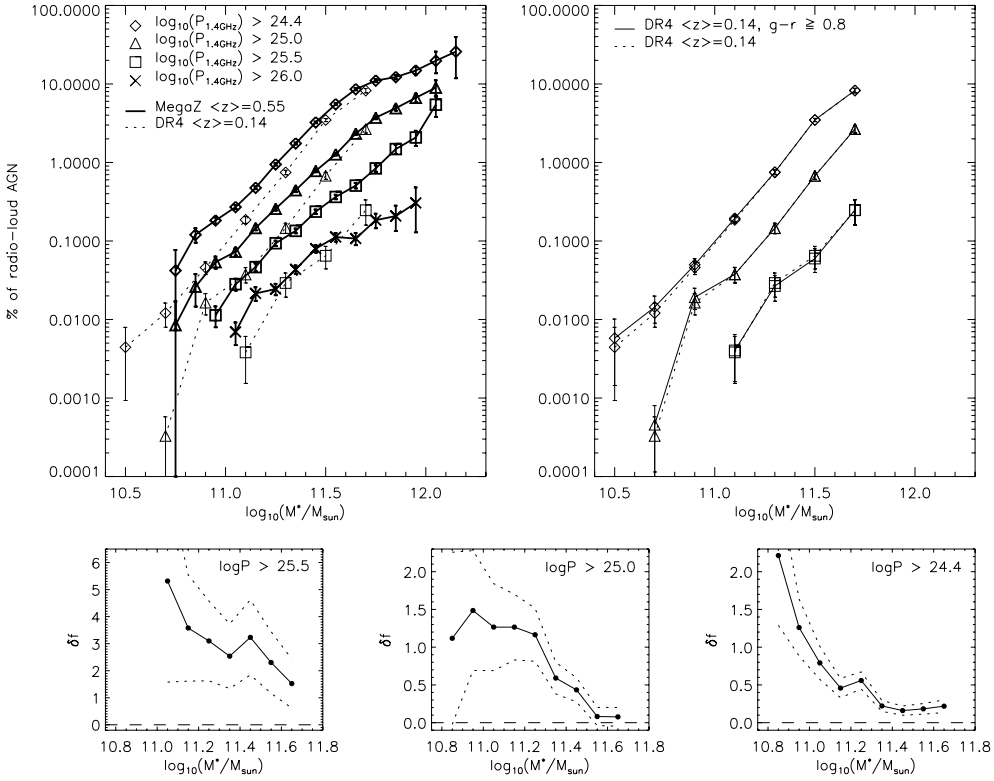

Figure 6. The left-hand upper panel shows the percentage of galaxies have radio luminosities above a given threshold, as a function of stellar mass. Results are shown for the high-redshift MegaZ-LRG sample (thick solid lines) and the low-redshift SDSS DR4 sample (thin dashed lines). The right-hand upper panel shows the radio-loud fractions for the SDSS DR4 sample, but including a colour constraint of $g - r \geq 0.8$. Lower panels show the relative variation δf between high-redshift (MegaZ) and low-redshift (DR4) radio-loud fractions as a function of stellar mass. Errors are poissonian and propagated via standard error propagation theory.

results to photo-z errors. Such errors could translate into systematic offsets in our estimates of stellar mass. In addition, the errors in the Sloan u, g, r, i, z magnitudes increase with redshift, so one might worry that this would translate into apparent (as opposed to real) evolution of the radio-loud fraction with redshift.

In order to test for such effects, we artificially redshifted our SDSS DR4 sample from their observed redshifts near $\langle z \rangle \sim 0.14$ out to the mean redshift of the MegaZ-LRG sample, $z = 0.55$. To do this, we applied the KCORRECT algorithm in conjunction with the e-corrections described above. We then added an error to the redshift using the distribution of $z_{\rm phot} - z_{\rm spec}$ of 2SLAQ galaxies. In practice, for each MegaZ-LRG, we extracted the 100 closest neighbours in g, r, i, z magnitude space in the 2SLAQ catalogue and we draw the redshift error, $z_{\rm phot} - z_{\rm spec}$, at random from this set of galaxies. Magnitude errors were assigned to each DR4 object in the same way. We then ran our code for estimating stellar mass on this 'artificially redshifted' data set, first applying just the redshift error, and secondly, incorporating errors on both the photometry and redshifts. The whole procedure was repeated 25 times. The solid line in Fig. 7 shows the difference between the mean fraction of radio-loud AGN measured in the 25 artificially redshifted samples and the 'true' value for the DR4 galaxies as a function of stellar mass. The difference δf is expressed in fractional terms, i.e. $\delta f = (\bar{F}_{\rm artificial} - F_{\rm true})/F_{\rm true}$. The shaded contours represent the 1σ scatter among the 25 samples. It can be seen that small systematic shifts in the derived radio-loud fractions do occur at the two ends of the stellar mass distributions. They also occur in our estimates of the fraction of the most luminous radio galaxies. On the whole, these effects are small (<20 per cent). Note that $10^{25.5}$ W Hz^{-1} sources are also much rarer in the DR4 catalogue than in the MegaZ sample, so the bottom right-hand panel overestimates the size of the true effect at this radio luminosity and is likely to apply only to very much higher luminosity cuts at $z = 0.55$.

3.5 Bivariate radio luminosity–mass function

The first determination of the bivariate radio-optical luminosity function was carried out by Auriemma et al. (1977) for a sample of 145 galaxies of type E and S0, and there were subsequent studies by Sadler, Jenkins & Kotanyi (1989) and Ledlow & Owen (1996). This (integrated) function measures the probability that a galaxy in a given optical absolute magnitude range hosts an AGN with radio power above a certain value. Best et al. (2005b) calculated the bivariate radio luminosity–stellar mass function of radio sources in the SDSS DR2, and parametrized the behaviour using a broken power with characteristic luminosity $P_\star = 2.5 \times 10^{24}$ W Hz^{-1}. A single fitting function was found to hold for all masses below $10^{11.5}\,{\rm M}_\odot$.

Our MegaZ radio galaxy sample is over 100 times larger than the one of Auriemma et al. (1977) and picks up close to the break luminosity found by Best et al. (2005b). Following Best et al. (2005b), we will use stellar mass instead of optical luminosity. We can thus interpret our calculation as the fraction of radio-loud AGN of a given mass emitting above a certain radio power. Fig. 8 shows the bivariate functions at high and low redshift in mass bins from 10^{11} to $10^{12.25}\,{\rm M}_\odot$. The most striking result shown in this plot is that

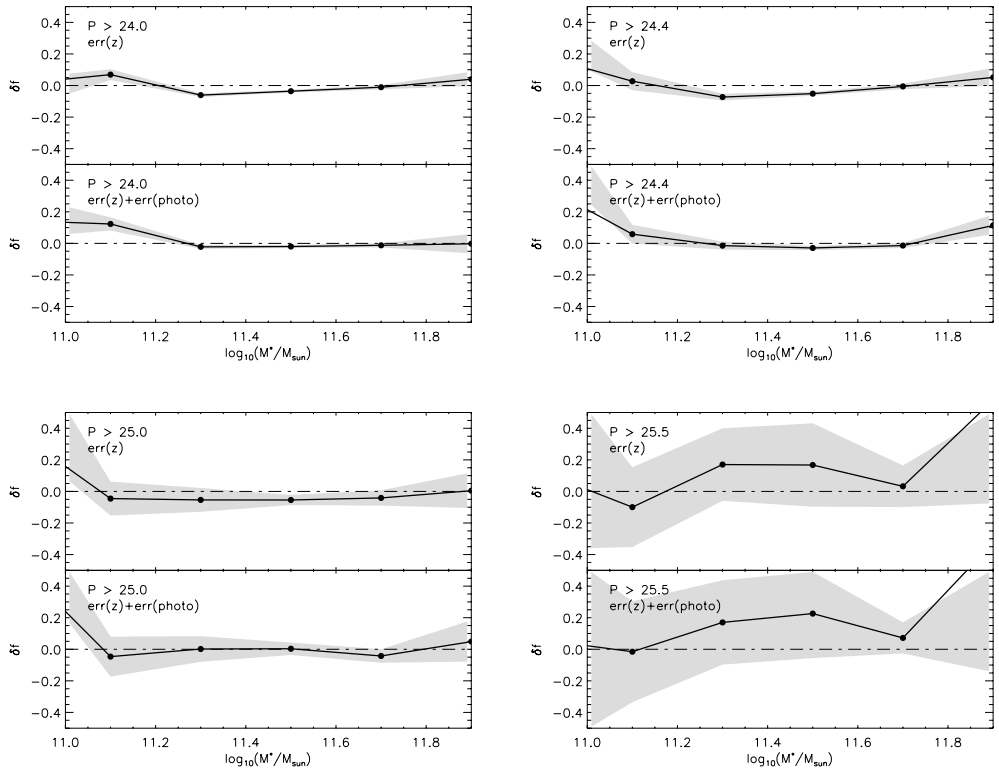

Figure 7. The difference between the true radio-loud AGN fraction and the one calculated for the artificially redshifted samples is plotted as function of stellar mass. Results are shown for increasing luminosity cuts. The solid line shows the mean difference for the 25 random samples, and the grey area is the 1σ scatter in this variation. Very few sources have masses higher than $10^{11.7}\,M_{\odot}$.

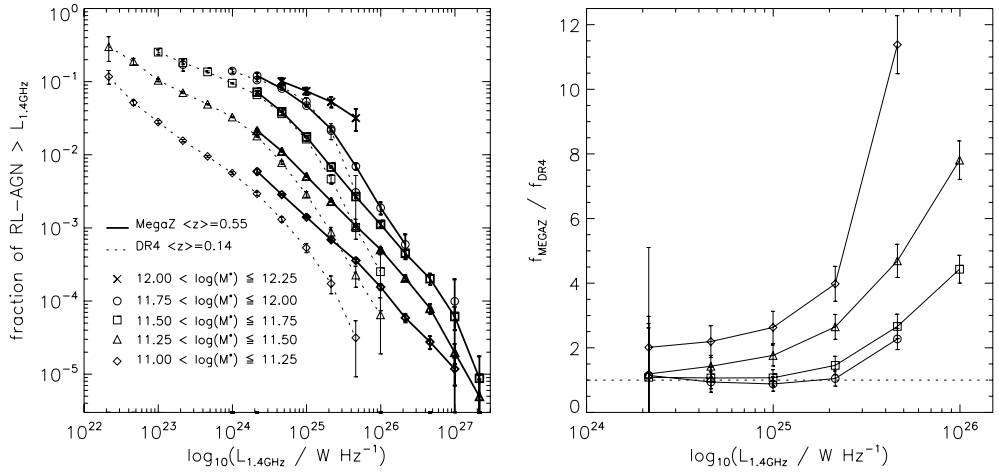

Figure 8. Integral bivariate radio luminosity–mass function in several bins of stellar mass (symbols) for high-redshift MegaZ-LRG sources (thick solid lines) and low-redshift SDSS DR4 sources (thin dashed lines). The bivariate function gives the fraction of radio-loud AGN brighter than a given radio luminosity, as a function of the luminosity. The right-hand panel shows the ratios of the bivariate functions derived for the MegaZ-LRG sample to those derived for the SDSS DR4 sample. These results show that radio sources evolve strongly across cosmic time depending on their stellar mass and radio luminosity. The dashed horizontal line marks the no-evolution scenario.

for galaxies of all stellar masses, the high-redshift fractions lie only slightly above the low redshift ones at faint radio luminosities, but there has been much stronger evolution at higher radio luminosities. This is shown in more detail in the right-hand panel of Fig. 8, where we plot the ratio of the radio-loud AGN fraction derived for the MegaZ-LRGs to that derived for the DR4 galaxies, as a function of radio power. We show results for the four mass bins for which there is a reasonable overlap between the two surveys (there are many fewer galaxies with $12 < \log M_* < 12.25$ in the DR4 sample, because the volume covered is much smaller.). It is striking that for all the mass bins, the ratio remains approximately constant up to a radio luminosity of 10^{25} W Hz^{-1} and then turns up sharply. As discussed in Section 1, 10^{25} W Hz^{-1} corresponds to the approximate dividing line between low- and high-excitation sources, and also

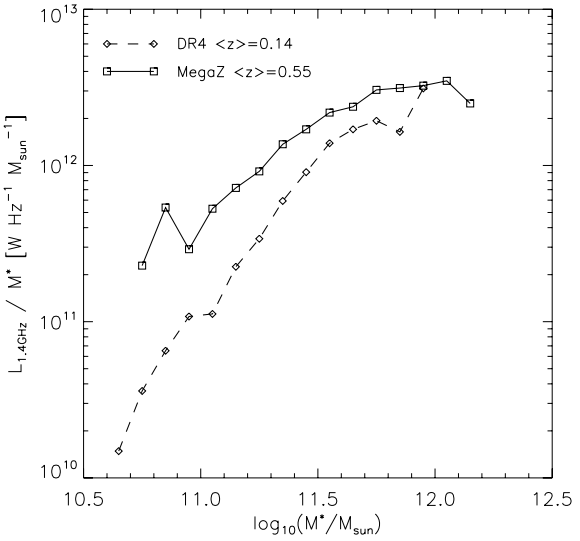

Figure 9. Integrated volume-weighted radio luminosity per unit stellar mass, as a function of stellar mass, for MegaZ-LRG radio-loud AGN (solid line with square symbols) and DR4 sources (dashed line with diamond symbols).

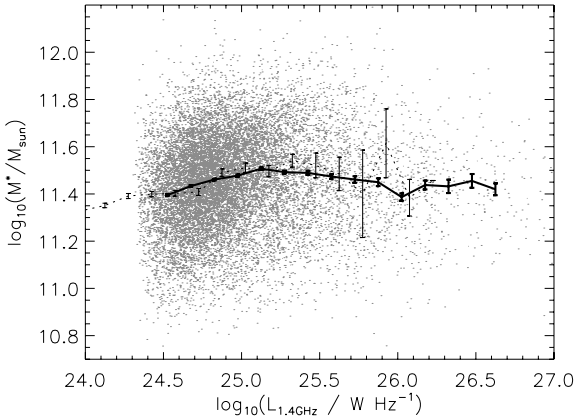

Figure 10. Median stellar mass of radio-loud AGN in the MegaZ-LRG (solid line) and SDSS DR4 (dotted line) samples as function of radio power. Grey dots represent the actual values for each MegaZ galaxy and errors are calculated by the bootstrapping technique.

delineates the boundary between strongly evolving and less strongly evolving radio sources found in previous studies. The main new result shown in this plot is that the strongest evolution in the radio source population apparently occurs *in the lowest mass galaxies*.

Another way of showing the same thing is to plot the integrated radio emission per unit stellar mass for galaxies of different stellar masses in the DR4 and MegaZ samples. Heckman et al. (2004) used the volume-weighted distribution of [O III] 5007 line luminosity per unit black hole mass to study the average rate at which black holes are accreting and growing. They find that low-mass black holes are currently growing at substantially higher rates than high-mass black holes. Best et al. (2005b) extended this analysis by computing the integrated radio luminosity per unit black hole mass, demonstrating that radio- and emission-line luminosities are produced in black holes of quite different masses (see fig. 11 in Best et al. 2005b).

In this work, we do not have direct estimates of black hole mass, so we carry out the computation as a function of stellar mass. In Fig. 9, we plot the volume-weighted radio luminosity per unit stellar mass, as a function of $\log M_*$, for our high- and low-redshift samples. The plot is constructed by taking at each mass bin, the ratio of the integrated (and weighted) radio luminosity, to the integrated (and weighted) stellar mass in that bin. As can be seen, radio activity has been boosted at all masses at high redshift, but the boost factor is considerably higher for low-mass galaxies.

4 THE STELLAR MASSES AND COLOURS OF THE HOST GALAXIES OF RADIO-LOUD AGN

It has long been known that powerful high-redshift radio galaxies are hosted by very massive galaxies with predominantly old stellar populations. This conclusion arises from the fact that there is a well-defined relation between the *K*-band magnitude of radio galaxies and redshift (the famous *K*–*z* relation) that agrees with the predictions of a passively evolving model galaxy of high mass ($>10^{11}$ $M_\odot$), and that there is relatively little scatter about this relation for the most luminous radio sources (e.g. Lilly & Longair 1985; Jarvis et al. 2001).

So far we have phrased our analysis of the relationship between radio AGN and their host galaxies in terms of the *probability* for a galaxy of a given mass to host such an AGN. We have shown that this *probability* evolves most strongly in low-mass galaxies. Note, however, that the fraction of radio-loud AGN is a strongly increasing function of galaxy mass both at $z = 0.55$ and 0.14. This means that radio galaxies in massive elliptical hosts always dominate *by number*.

This is shown in more detail in Fig. 10, where we plot the median stellar masses of both the MegaZ and SDSS DR4 radio AGN as a function of radio luminosity. As can be seen, radio AGN are hosted by galaxies with median masses of $\sim 3 \times 10^{11}$ $M_\odot$ in both the surveys. There is a weak increase in the median mass at higher radio luminosities.

In Fig. 11, we plot the colour distributions of the MegaZ radio AGN. One must, of course, bear in mind that the MegaZ sample is selected so as to occupy a restricted range in colour space, but we can nevertheless check whether there are any colour differences between different types of radio AGN. We split the sample into three different redshift bins and show results for low-luminosity ($<10^{25.3}$ W Hz^{-1}) and high-luminosity ($>10^{25.3}$ W Hz^{-1}) radio sources. As was found previously by Smith & Heckman (1989), there is a tendency for the more powerful radio galaxies to have slightly bluer colours at fixed redshift, but the effect is very weak.

In summary, we conclude that the majority of both low- and high-luminosity radio AGN are hosted by massive (3 L_*) galaxies with red colours. This is in good agreement with past work on this subject.

5 SUMMARY AND DISCUSSION

The main results of this work can be summarized as follows.

A catalogue of 14 453 radio-loud AGN with 1.4 GHz fluxes above 3.5 mJy in the redshift range $0.4 < z < 0.8$, has been constructed from the cross-correlation of NVSS and FIRST radio source catalogues with the MegaZ-LRG catalogue of LRGs. The vast majority of the radio AGN are single component sources in both NVSS and FIRST. However, there is a significant fraction of objects without high signal-to-noise ratio (S/N) FIRST detections, which are required for accurate identification of the optical counterpart. We thus introduced a method for analysing the FIRST radio maps around the

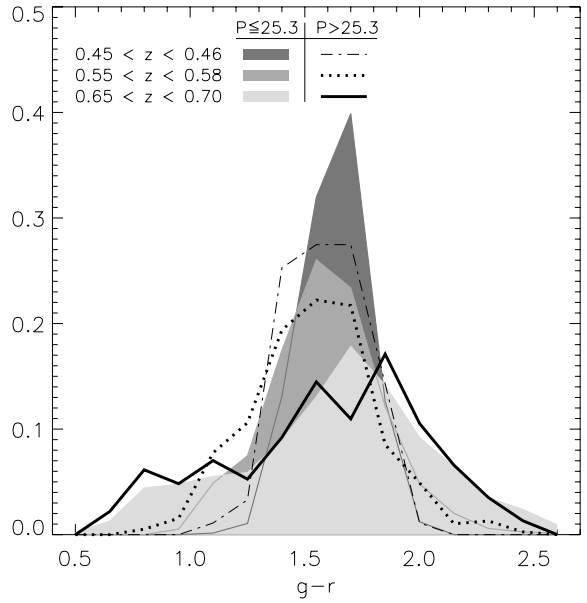

Figure 11. Colour distribution of MegaZ-LRG in three different redshift bins, split into a high-luminosity population of radio sources with $\log_{10}[P_{1.4\,GHz}/(W\ Hz^{-1})] \leq 25.3$, and a low-luminosity population with $\log_{10}[P_{1.4\,GHz}/(W\,Hz^{-1})] > 25.3$.

candidate positions of these sources. This allowed us to dig deeper into the FIRST survey and use lower S/N detections to pinpoint the location of the host galaxy.

We have presented a new determination of the luminosity function of radio-loud AGN at $z \sim 0.55$ that is in excellent agreement with other results in the literature, but with notably smaller error bars. By comparing our radio luminosity function at $z \sim 0.55$ to that derived for a large sample of nearby radio AGN from the SDSS DR4, we find compelling evidence for strong cosmic evolution of radio sources. The comoving number density of radio AGN with luminosities less than 10^{25} W Hz^{-1} increases by a factor of $\sim$1.5 between $z = 0.14$ and 0.55. At higher luminosities, this factor increases sharply, reaching values $\sim$10 at a radio luminosity of 10^{26} W Hz^{-1}. Neither a pure luminosity evolution nor a pure density evolution scenario provides a good description of the data.

We then turn to an analysis of how the relation between radio AGN and their host galaxies evolves with redshift. The fraction of galaxies with radio luminosities above a given threshold is a steeply increasing function of stellar mass at both $z \sim 0.1$ and 0.55. The fraction of radio-loud AGN increases with redshift and this increase is largest at the highest radio luminosities and also for lower mass galaxies. We have also calculated the bivariate radio luminosity–mass function at $z \sim 0.14$ and 0.55. Its shape does not appear to depend on mass at either redshift, but there is strong evolution in the shape at the *bright-end* of the function. The fraction of galaxies brighter than 10^{25} W hz^{-1} declines with significantly shallower slope at higher redshifts. Within the range 10^{25-27} W hz^{-1}, simple power-law fits to the DR4 bivariate function in Fig. 8 (frac $\propto L_{1.4\,GHz}^{\gamma}$), produce slopes γ of -1.84 ± 0.21, -1.66 ± 0.02 and -1.83 ± 0.04 for the first, second and third mass bins. In MegaZ, we obtain -1.05 ± 0.02, -1.16 ± 0.05 and -1.20 ± 0.02 for the same luminosity range and mass bins.

In short, two main conclusions have emerged from our analysis.

(i) There is a characteristic luminosity of $\sim 10^{25}$ W Hz^{-1} below which the radio source population appears to evolve only very weakly with redshift. Above this characteristic luminosity, there is a strong evolution, with the most powerful radio sources undergoing the largest increase in co-moving number density. These results are in broad agreement with past studies.

(ii) The strongest evolution in the fraction of galaxies that host radio-loud AGN takes place in the lower mass galaxies in our sample.

The most plausible explanation of these trends is that there are two classes of radio galaxy, likely associated with the high excitation/low excitation 'dichotomy') that have different fuelling/triggering mechanisms and hence evolve in different ways. This has also been argued by Tasse et al (2008), whose analysis of a sample 1 per cent of the size of ours in the XMM–LSS region provided hints of similar evolutionary properties. As discussed before, it has been hypothesized that the class of low-luminosity AGN is likely associated with massive ($\sim 10^{13}$ M$_\odot$) dark matter haloes with quasi-static hot gas atmospheres. The abundance of such haloes is predicted to remain approximately constant out to redshifts $\sim$1 (Mo & White 2002) and this is broadly consistent with the very weak evolution we see in this population. These 'hot-halo' triggered sources at $z \sim 0.5$ would then produce radio emission that roughly compensates the radiative losses of the hot gas.

The reason for the remarkably strong evolution in the comoving abundance of high-luminosity radio AGN is somewhat more difficult to understand. As shown in Fig. 8, this evolution is most dramatic in galaxies at the low stellar mass end of our sample. It is thus tempting to link this population with the strongly accreting (and evolving) population of luminous quasars, whose space densities also increase by factors of more than 10 over the redshift range studied in this paper. Recent work has shown that quasars are hosted in dark matter haloes of masses $\sim 10^{12}$ M$_\odot$, independent of redshift or the optical luminosity of the system (e.g. Croom et al. 2005; Shen et al. 2007). Only $\sim$10 per cent of optical quasars are radio loud, however, and this raises the question as to whether there is simply a short radio-loud phase during the lifetime of every optical quasar, or whether optically luminous AGN and powerful radio galaxies are triggered under different physical conditions. If, as in quasars, these sources are not regulated by cooling from a surrounding hot gaseous halo, but by other mechanisms like interactions/mergers, then we would not expect to find them in an equilibrium state like in low excitation AGN.

One way to shed further light on these matters is to compare the clustering properties of quasars to those of the luminous radio galaxies in our sample. If their clustering properties are identical, this would favour the hypothesis that all quasars experience a radio-loud phase. Recently, Kauffmann, Heckman & Best (2008) found that nearby radio-loud AGN were more strongly clustered than matched samples of radio-quiet AGN with the same black hole masses and extinction corrected [O III] line luminosities. It will be interesting to see if the same conclusion holds at higher redshifts and for more powerful systems. This will be the subject of a future paper.

ACKNOWLEDGMENTS

We would like to thank the Max Planck Society for the financial support provided through its Max Planck Research School on Astrophysics PhD program. We also thank T. Heckman, C. Li, V. Wild and N. Drory, as well as the anonymous referee, for valuable support and suggestions. The research uses the SDSS Archive, funded by the Alfred P. Sloan Foundation, the Participating Institutions, the

National Aeronautics and Space Administration, the National Science Foundation, the US Department of Energy, the Japanese Monbukagakusho and the Max Planck Society. The research project uses the NVSS and FIRST radio surveys, carried out using the National Radio Astronomy Observatory Very Large Array. NRAO is operated by Associated Universities Inc., under cooperative agreement with the National Science Foundation.

REFERENCES

Auriemma C. G., Perola G., Ekers R., Fanti R., Lari C., Jaffe W., Ulrich M., 1977, A&A, 57, 41
Barthel P. D., 1989, ApJ, 336, 606
Becker R. H., White R. L., Helfand D. J., 1995, ApJ, 450, 559
Best P. N., Kauffmann G., Heckman T. M., Brinchmann J., Charlot S., Ivezić Ž., White S. D. M., 2005b, MNRAS, 362, 25
Best P. N., Kauffmann G., Heckman T. M., Ivezić Ž., 2005a, MNRAS, 362, 9
Best P. N., Kaiser C. R., Heckman T. M., Kauffmann G., 2006, MNRAS, 368, L67
Bicknell G. V., 1995, ApJS, 101, 29
Blanton M. R., Roweis S., 2007, AJ, 133, 734
Böhringer H., Voges W., Fabian A. C., Edge A. C., Neumann D., 1993, MNRAS, 264, L25
Bower R. G., Benson A. J., Malbon R., Helly J. C., Frenk C. S., Baugh C. M., Cole S., Lacey C. G., 2006, MNRAS, 370, 645
Brown M. J. I., Webster R. L., Boyle B. J., 2001, AJ, 121, 2381
Brown M. J. I., Dey A., Jannuzi B. T., Brand K., Benson A. J., Brodwin M., Croton D. J., Eisenhardt P. R., 2007, ApJ, 654, 858
Bruzual G., Charlot S., 2003, MNRAS, 344, 1000
Budavári T., Dobos L., Szalay A. S., Greene G., Gray J., Rots A. H., 2007, in Shaw R. A., Hill F., Bell D. J., eds, Proc. ASP Conf. Ser. 376, Astronomical Data Analysis Software and Systems. Astron. Soc. Pac., San Francisco, p. 559
Cannon R. D. et al., 2006, MNRAS, 372, 425
Clewley L., Jarvis M. J., 2004, MNRAS, 352, 909
Cole S., Lacy C. G., Baugh C. M., Frenk C. S., 2000, MNRAS, 319, 168
Colless M. M. et al., 2001, MNRAS, 328, 1039
Collister A. A., Lahav O., 2004, PASP, 116, 345
Collister A. et al., 2007, MNRAS, 375, 68
Condon J. J., Cotton W. D., Greisen E. W., Yin Q. F., Perley R. A., Taylor G. B., Broderick J. J., 1998, AJ, 115, 1693
Condon J. J., Cotton W. D., Broderick J. J., 2002, AJ, 124, 675
Cool R. J. et al., 2008, ApJ, 682, 919
Croom S. M. et al., 2005, MNRAS, 356, 415
Croton D. et al., 2006, MNRAS, 365, 11
Dunlop J. S., Peacock J. A., 1990, MNRAS, 19, 42
Fabian A. C., Sanders J. S., Allen S. W., Crawford C. S., Iwasawa K., Johnstone R. M., Schmidt R. W., Taylor G. B., 2003, MNRAS, 344, L43
Fanaroff B. L., Riley J. M., 1974, MNRAS, 167, 31
Fukugita M., Ichikawa T., Gunn J. E., Doi M., Shimasaku K., Schneider D. P., 1996, AJ, 111, 1748
Gunn et al., 1998, AJ, 116, 3040
Hardcastle M. J., Evans D. A., Croston J. H., 2007, MNRAS, 376, 1849
Heckman T. M., Kauffmann G., Brinchmann J., Charlot S., Tremonti C., White S. D. M., 2004, ApJ, 613, 109
Heywood I., Blundell K. M., Rawlings S., 2007, MNRAS, 381, 1093
Jackson C. A., Wall J. V., 1999, MNRAS, 304, 160
Jarvis M. J., Rawlings S., Eales S., Blundell K. M., Bunker A. J., Croft S., McLure R. J., Willott C. J., 2001, MNRAS, 326, 1585
Kauffmann G. et al., 2003, MNRAS, 341, 33
Kauffmann G., Heckman T. M., Best P. N., 2008, MNRAS, 384, 953
Ledlow M. J., Owen F. N., 1996, AJ, 112, 1
Li C., Kauffmann G., Jing Y. P., White S. D. M., Börner G., Cheng F. Z., 2006, MNRAS, 368, 21
Lilly S. J., Longair M. S., 1985, MNRAS, 211, 833
Longair M. S., 1966, MNRAS, 133, 421
McNamara B. R. et al., 2000, ApJ, 534, L135
Mo H. J., White S. D. M., 2002, MNRAS, 336, 112
Obric M. et al., 2006, MNRAS, 370, 1677
Ross N. P. et al., 2007, MNRAS, 381, 573
Sadler E. M., Jenkins C. R., Kotanyi C. G., 1989, MNRAS, 240, 591
Sadler E. M. et al., 2002, MNRAS, 329, 227
Sadler E. M. et al., 2007, MNRAS, 381, 211
Schlegel D. J., Finkbeiner D. P., Davis M., 1998, ApJ, 500, 525
Schmidt M., 1968, ApJ, 151, 393
Shen Y. et al., 2007, AJ, 133, 2222
Smith E. P., Heckman T. M., 1989, ApJ, 341, 658
Stoughton C. et al., 2002, AJ, 123, 485
Tabor G., Binney J., 1993, MNRAS, 263, 323
Tasse C., Best P. N., Röttgering H., Le Borgne D., 2008, A&A, in press
Wake D. A. et al., 2006, MNRAS, 372, 537
White S. D. M., Frenck C. S., 1991, ApJ, 379, 52
York D. G. et al., 2000, AJ, 120, 1579

This paper has been typeset from a TEX/LATEX file prepared by the author.